

## Turbulence and star formation in molecular clouds

Richard B. Larson *Yale University Observatory, Box 6666, New Haven, Connecticut 06511, USA*

Received 1980 July 7; in original form 1980 May 7

**Summary.** Data for many molecular clouds and condensations show that the internal velocity dispersion of each region is well correlated with its size and mass, and these correlations are approximately of power-law form. The dependence of velocity dispersion on region size is similar to the Kolmogoroff law for subsonic turbulence, suggesting that the observed motions are all part of a common hierarchy of interstellar turbulent motions. The regions studied are mostly gravitationally bound and in approximate virial equilibrium. However, they cannot have formed by simple gravitational collapse, and it appears likely that molecular clouds and their substructures have been created at least partly by processes of supersonic hydrodynamics. The hierarchy of subcondensations may terminate with objects so small that their internal motions are no longer supersonic; this predicts a minimum protostellar mass of the order of a few tenths of a solar mass. Massive ‘protostellar’ clumps always have supersonic internal motions and will therefore develop complex internal structures, probably leading to the formation of many pre-stellar condensation nuclei that grow by accretion to produce the final stellar mass spectrum. Molecular clouds must be transient structures, and are probably dispersed after not much more than  $10^7$  yr.

### 1 Introduction

There is much evidence that stars form in the interiors of dense, gravitationally bound molecular clouds, but little is yet known about the detailed internal structure and dynamics of such clouds, or about the processes by which stars form in them. This lack of direct information has allowed theorists considerable scope for calculating idealized models for the collapse and fragmentation of gas clouds, starting with simple assumed initial conditions (see the reviews by Larson 1977a; Woodward 1978; Bodenheimer & Black 1978). Much of this work has been motivated by the ‘gravitational instability’ picture of star formation elaborated by Jeans (1929), Hoyle (1953) and Hunter (1967), whereby diffuse clouds that are initially nearly uniform collapse and fragment into a hierarchy of successively smaller condensations as the density rises and the Jeans mass decreases.

In several respects, however, the properties of molecular clouds are not consistent with this simple classical picture. For example, no large, nearly uniform, and quiescent clouds that might be in early stages of fragmentation have been observed; all large molecular clouds are quite inhomogeneous and clumpy, frequently showing structure on the smallest resolvable scales. Moreover, all but the smallest clouds have supersonic internal motions of a more-or-less chaotic nature, which would generate strong density inhomogeneities even if none were present initially. The probable role of complex hydrodynamical processes in structuring molecular clouds is also suggested by the filamentary and windswept appearance of objects like the Taurus dark clouds, which is suggestive of turbulent flows. Some dark clouds projected in front of bright backgrounds such as the North America nebula show extremely wispy structures with features as small as can be resolved on photographs, i.e. several arcsec or  $\sim 10^{-2}$  pc; this is smaller than any likely value of the Jeans length in dark clouds, so these features are not likely to have a purely gravitational origin.

Many efforts have been made to interpret molecular line profiles in terms of idealized models for the internal kinematics of molecular clouds, but this has remained a controversial subject, and it has not been possible to decide whether the dominant form of motion is collapse, rotation, small-scale random motions, or random motions of large blobs (Zuckerman & Palmer 1974; Penzias 1975; Field 1978; Evans 1980). Most likely the real situation is more complex than any of the models, and all of the proposed effects play a role. Since the observed motions are in any case always irregular to some extent, it seems reasonable to describe them as turbulent; in fact, no sharp distinction can really be drawn between 'systematic motions' and 'turbulence', because turbulent flows actually consist of a hierarchy of small-scale irregularities superimposed on larger-scale, more systematic motions. The important feature of such flows is the relative magnitude of the small-scale and large-scale motions, i.e. the spectrum of characteristic velocities as a function of the length scale.

A previous study of the spectrum of interstellar motions by Larson (1979) showed, on the basis of limited data, that the velocity dispersion increases systematically with region size, following an approximate power-law dependence that is not greatly different from the Kolmogoroff law for subsonic turbulence. This suggests that all of the motions considered, including those in molecular clouds, are part of a common hierarchy of interstellar turbulent motions. In Sections 2 and 3, the question of whether the motions in molecular clouds follow a common power-law relation between velocity dispersion and region size will be re-examined on the basis of much more data.

Many molecular clouds are observed to contain or consist of a number of clumps with independent, apparently random motions (e.g. Crutcher, Hartkopf & Giguere 1978; Blitz 1980). In some cases, such as the well-studied  $\rho$  Oph cloud, there is a hierarchy of smaller and denser clumps embedded in larger, more diffuse ones (Myers *et al.* 1978). A question of importance for star formation is whether these substructures in molecular clouds are all gravitationally bound; if so, the smallest and densest ones may play a direct role in star formation, or may represent protostars. Since the internal motions in the clumps are almost always supersonic, these motions provide the dominant form of support against gravity. In order to examine in Section 4 whether molecular clouds and subcondensations of various sizes are in approximate virial equilibrium, and to study in Section 5 the density structure of molecular clouds, we consider in this paper only clouds for which mass determinations are available.

If protostars form as part of a hierarchy of bound substructures in molecular clouds, their properties will depend on the overall spectra of density and velocity fluctuations in molecular clouds. This may have important implications for star formation and the stellar

mass spectrum; for example, if there is a minimum size of bound condensations produced by supersonic compression processes, this may lead to a lower limit of stellar masses. If larger 'protostellar' condensations always have supersonic internal motions and large density inhomogeneities, this will require revision of simple collapse models, perhaps in the direction of the 'floccule' theory of McCrea (1960). These possible implications of turbulence in molecular clouds for star formation will be considered further in Section 6. Possible implications for the evolution and longevity of molecular clouds will be considered in Section 7.

## 2 Basic data on molecular clouds

To determine the internal velocity dispersion as a function of region size, it is necessary to know the maximum linear extent  $L$  of each region and the variation across it of both the radial velocity  $V$  and the linewidth  $\Delta V$ , so that the three-dimensional velocity dispersion  $\sigma$  due to all motions present can be calculated. The regions considered here include cloud complexes, individual clouds (which may be parts of larger complexes) and clumps or density enhancements in larger clouds. In order to investigate whether the virial theorem is satisfied, attention has been restricted to clouds or complexes for which mass estimates not based on the virial theorem are available, although to provide more complete information on some complexes, data have been included for parts of them for which no individual mass estimates are available.

In order to minimize effects of line saturation, which make it difficult or impossible to obtain the true velocity dispersion from the linewidth (Phillips *et al.* 1979), optically thick lines have been avoided wherever possible and used only in a few cases where large-scale velocity variations across the cloud provide the dominant contribution to the velocity dispersion. In practice, this means that observations of the  $^{12}\text{CO}$  molecule have generally not been used, and the data used here are based mostly on observations of  $^{13}\text{CO}$ . Also, to a lesser extent, data for  $\text{H}_2\text{CO}$ ,  $\text{NH}_3$ ,  $\text{OH}$ ,  $\text{HC}_3\text{N}$ ,  $\text{HC}_5\text{N}$ ,  $\text{SO}$ ,  $\text{HCO}^+$  and  $\text{HI}$  have been used.

Table 1 lists most of the regions for which data satisfying the above requirements were found in the literature of approximately 1974–79. Also listed in Table 1 are the molecule(s) studied in each case, the symbol representing each region in subsequent figures, various basic and derived parameters to be explained below, and references for the sources of the data. In a number of cases, data for regions with similar properties have been averaged into a single entry in the table.

The region size  $L$ , given in parsecs in Table 1, is approximately the maximum projected dimension of the region in which the molecule observed was detected or mapped. For a clump in a larger cloud, the indicated size is approximately that of the largest closed map contour defining the clump. In many cases the edges of the clouds are ragged or not well defined by the available data, so their sizes are somewhat uncertain. Including errors in the distances of the clouds, the uncertainties in the values of  $L$  in Table 1 are estimated to be typically 20–50 per cent.

The estimated total mass  $M$  of each region, listed in solar masses in Table 1, is generally quoted directly from the references, or averaged from different determinations. For most of the clouds with  $^{13}\text{CO}$  data, i.e. most of the larger clouds, the masses are based on the usual assumptions that the ratio of the column density of  $^{13}\text{CO}$  to that of  $\text{H}_2$  is  $2 \times 10^{-6}$  (Dickman 1978), and that  $\text{H}_2$  constitutes 70 per cent of the total mass. In a few cases where authors have used different assumptions, their results have been revised to make them consistent with the above assumptions. For objects lacking  $^{13}\text{CO}$  data and for dense regions where  $^{13}\text{CO}$  is not a good probe, the masses have generally been estimated from the densities required

**Table 1.** Basic data for molecular clouds and condensations.  $L$  is the maximum linear dimension,  $M$  the total mass,  $\sigma$  the three-dimensional rms internal velocity, and  $\langle n(\text{H}_2) \rangle$  the average space density of  $\text{H}_2$  molecules in each region.

Object	Molecule	Plot symbol	$L$ (pc)	$M$ ( $M_\odot$ )	$\sigma$ (km/s)	$\frac{2GM}{\sigma^2 L}$	$\langle n(\text{H}_2) \rangle$	Ref.
Orion complex:								
L1641 (Ori A)	$^{12}\text{CO}$	0	65	100000	5.5	0.46	10	1
L1641 clumps N,S	$\text{H}_2\text{CO}$	0	10	14000	2.5	2.0	390	2
OMC1	$\text{NH}_3, ^{13}\text{CO}$	0	1.2	1000	2.5	1.20	16000	3,4
OMC2	$\text{NH}_3$	0	0.5	100	1.1	1.49	22000	3
KL infrared neb.	$\text{NH}_3$	0	0.05		2.2			5
L1630 (Ori B)	$^{13}\text{CO}$	0	25	60000	1.9	6.0	110	6,1
NGC 2023-24	$^{13}\text{CO}$	0	5		1.9			6
NGC 2068	$^{13}\text{CO}$	0	3		1.3			6
Ori-1-2	$^{13}\text{CO}$	0	0.25	6	0.95	0.22	9800	7
ML7 (Ser OB1) complex:								
ML7 cloud	$^{13}\text{CO}$	M	130	300000	3.7	1.52	4	8
clumps C,D	$^{13}\text{CO}$	M	11	40000	3.3	3.0	840	8
clumps A,B	$^{13}\text{CO}$	M	5	30000	2.8	6.9	6700	8
region III	$^{13}\text{CO}$	M	7	20000	2.0	6.4	1600	8
ML7SW(core of B)	$^{13}\text{CO}, \text{NH}_3$	M	3	10000	3.5	2.5	10000	9
W3 (Cas OB6) complex:								
W3-4 cloud	$^{13}\text{CO}$	W	60	100000	8.5	0.21	13	10
W3-4 clumps I-III	$^{13}\text{CO}$	W	8	10000	3.1	1.17	540	10
Per OB2 complex:								
Per OB2 cloud	$^{12}\text{CO}$	P	35	40000	4.4	0.53	26	11
NGC 1333	$^{13}\text{CO}$	P	3		2.3			12
B205	$\text{NH}_3$	P	0.6	40	0.8	0.94	5200	13
Cep OB3 complex:								
region ABC	$^{13}\text{CO}$	C	25	5000	3.0	0.20	9	14,11
clumps A,B,C	$^{13}\text{CO}$	C	3	500	2.0	0.38	520	14,11
HII regions:								
NGC 7538	$\text{H}_2\text{CO}$	N	50	200000	5.5	1.19	45	15
NGC 2264	$^{13}\text{CO}$	N	15	20000	3.5	0.98	170	16
" clumps A-H	$^{13}\text{CO}$	N	1.8	800	1.9	1.11	3800	16
" clouds B,C	$\text{H}_2\text{CO}$	N	2.1	300	1.7	0.44	900	17
NGC 6334	$^{13}\text{CO}$	N	8	14000	4.4	0.81	760	18
S106 cloud	$^{13}\text{CO}$	S	15	30000	2.8	2.3	250	19
" core region	$\text{NH}_3$	S	6		1.3			20
S255	$^{13}\text{CO}$	S	5	1500	2.1	0.61	330	21
S140	$^{13}\text{CO}$	S	4.5	2300	2.2	0.95	700	22
$\rho$ Ophiuchus complex:								
$\rho$ Oph cloud	HI	$\rho$	20		2.4			23
" frag. 4	$\text{H}_2\text{CO}$	$\rho$	2.0	400	1.25	1.15	1400	23
" frag. 1,2	$\text{H}_2\text{CO}$	$\rho$	0.8	120	1.0	1.35	6500	23
" clump	SO	$\rho$	0.4		0.9			23
" clump	$\text{HCO}^+$	$\rho$	0.25		0.8			23
Taurus complex:								
Taurus clouds	$\text{H}_2\text{CO}, ^{13}\text{CO}$	T	18	4000	1.7	0.69	19	24,25
Cloud 2 (B22)	OH, HI	T	3	1000	1.1	2.5	1000	26,27
B7, B19	OH, $\text{NH}_3$	T	1.0	140	0.95	1.40	3900	13
TMC1	$\text{HC}_3\text{N}$	T	0.2	2	0.40	0.56	7000	28
TMC2	$\text{HC}_5\text{N}, \text{NH}_3$	T	0.1	1	0.35	0.73	28000	29
Stars, all		*	36		4.7			30

Table 1 – continued

Object	Molecule	Plot symbol	L (pc)	M ( $M_{\odot}$ )	$\sigma$ (km/s)	$\frac{2GM}{\sigma^2 L}$	$\langle n(H_2^2) \rangle$	Ref.
Stars, group II		*	12		3.4			30
Stars, group I		*	4		1.8			30
Reflection nebulae:								
Mon R2	$^{13}CO$	R	7	8000	2.6	1.52	650	31
NGC 7023	$^{13}CO$	R	5	600	1.4	0.55	130	32
R CrA	$^{13}CO$	R	2.3	2500	1.3	5.8	5700	33
NGC 7129	$^{13}CO$	R	1.5	200	1.4	0.61	1700	34
Lynds dark clouds:								
L134	$^{13}CO, OH$	L	0.8	100	0.75	2.0	5400	7, 35
L134N	$^{13}CO$	L	1.4	100	1.4	0.33	1000	36, 37
L43	$^{13}CO$	L	1.1	15	0.70	0.25	310	38
L1551, 134N, 1235	$H_2CO$	L	0.23	29	0.75	2.0	66000	36
L1544, L63	$H_2CO$	L	0.18	10	0.65	1.18	48000	36
L1407, L1257	$H_2CO$	L	0.12	6	0.86	0.61	97000	36
Barnard objects:								
B227	$^{13}CO$	B	0.70	18	0.92	0.27	1500	7
B335	$^{13}CO$	B	0.63	31	0.67	0.99	3500	7
B163	$^{13}CO$	B	0.46	21	0.80	0.64	6000	7
B68	$^{13}CO$	B	0.22	1.6	0.53	0.23	4200	7

## References

- Kutner *et al.* (1977)
- Few & Booth (1979)
- Ho *et al.* (1979)
- Liszt *et al.* (1974)
- Wilson *et al.* (1979)
- Milman (1975)
- Martin & Barrett (1978)
- Elmegreen *et al.* (1979)
- Lada (1976)
- Lada *et al.* (1978)
- Sargent (1979)
- Loren (1976)
- Lang & Willson (1979)
- Sargent (1977)
- Minn & Greenberg (1975)
- Crutcher *et al.* (1978)
- Minn & Greenberg (1979)
- Dickel, Dickel & Wilson (1977)
- Lucas *et al.* (1978)
- Little *et al.* (1979)
- Evans, Blair & Beckwith (1977)
- Blair *et al.* (1978)
- Myers *et al.* (1978)
- Heiles & Katz (1976)
- Stark & Blitz (1978)
- Heiles & Gordon (1975)
- Wilson & Minn (1977)
- Churchwell, Winnewisser & Walmsley (1978)
- Myers *et al.* (1979)
- Jones & Herbig (1979)
- Loren (1977)
- Elmegreen & Elmegreen (1978)
- Loren (1979)
- Bechis *et al.* (1978)
- Mattila, Winnberg & Grasshoff (1979)
- Snell (1979)
- Caldwell (1979)
- Elmegreen & Elmegreen (1979)

to produce the observed molecular excitation, together with simple assumptions about the geometry, such as uniform spherical or prolate-spheroidal shapes. The mass estimates listed in Table 1 are probably uncertain by a factor of 2 in typical cases, but errors of a factor of 4 or more cannot be ruled out in some cases.

The velocity dispersion  $\sigma$  listed in Table 1 is the total three-dimensional rms velocity of all internal motions in each region, and has been calculated by adding the contributions to  $\sigma^2$  due to (1) large-scale velocity variations across the region, (2) the smaller-scale motions responsible for the linewidth, and (3) thermal motions. The thermal contribution is significant only for a few of the smallest objects in which  $\sigma < 1 \text{ km s}^{-1}$ , and has been assumed

to be  $\sigma_s = 0.32 \text{ km s}^{-1}$ , as appropriate for molecular gas at a temperature of 10 K. In deriving three-dimensional velocity dispersions from the observed radial velocities and linewidths it has always been assumed that the velocity distribution is isotropic. In most regions the dominant contribution to  $\sigma$  comes from the linewidth and thus from relatively small-scale motions, so that the assumption of an isotropic velocity distribution may be reasonable; however, for some of the largest clouds the dominant contribution to  $\sigma$  comes from systematic velocity variations across the cloud, and the assumption of an isotropic velocity distribution can be valid only as an average over many clouds. The uncertainty in  $\sigma$  is estimated to be of the order of 20 per cent for most clouds, but the error could be as large as 50 per cent or more for some of the largest clouds, for the reason just mentioned.

### 3 Turbulence in molecular clouds

The velocity dispersion  $\sigma$  is plotted logarithmically versus region size  $L$  in Fig. 1, which includes all of the objects for which a mass estimate is given in Table 1. A well-defined correlation between  $\log \sigma$  and  $\log L$  is seen, and within the scatter it is well represented by the eye-fitted dashed straight line, whose equation is

$$\sigma(\text{km s}^{-1}) = 1.10 L(\text{pc})^{0.38}. \quad (1)$$

The rms deviation of  $\log \sigma$  from this relation is 0.14, corresponding to a factor of 1.38 in  $\sigma$ . Equation (1) holds for  $0.1 \lesssim L \lesssim 100 \text{ pc}$ , and is almost identical to the relation  $\sigma = 1.1 L^{0.37}$  found by Larson (1979) for interstellar motions on somewhat larger length scales,  $1 \lesssim L \lesssim 1000 \text{ pc}$ ; this earlier study included fewer data on molecular clouds, but some data on H I cloud velocities and larger-scale streaming motions. The present result strengthens the conclusion that the velocity dispersion of interstellar motions shows a general power-law correlation with region size, and extends it to smaller length scales.

The data in Table 1 show, moreover, that a similar relation between  $\sigma$  and  $L$  often holds even within individual clouds. Fig. 2 shows the variation of  $\sigma$  with  $L$  in all of the clouds or complexes for which at least one subregion is listed in Table 1; in this diagram straight lines connect the symbols for each subregion and the larger cloud of which it is a part. The velocity dispersions of groups of T Tauri stars in the Taurus clouds (Table 1 and Jones & Herbig 1979) are also plotted as asterisks in Fig. 2(a). The left part of Fig. 2(b) shows additional data for several dark clouds as reproduced from Fig. 89 of Snell (1979); in this

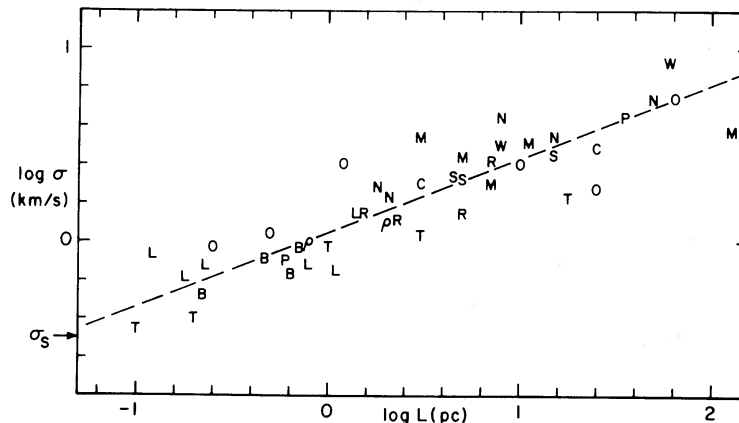
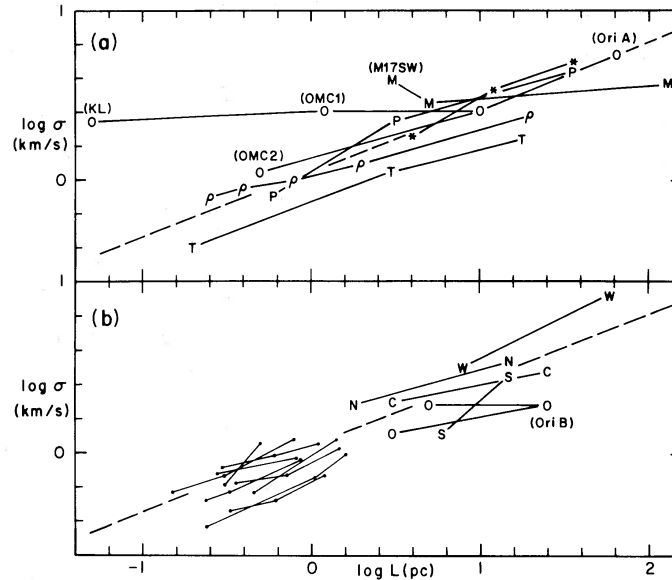


Figure 1. The three-dimensional internal velocity dispersion  $\sigma$  plotted versus the maximum linear dimension  $L$  of molecular clouds and condensations, based on data from Table 1; the symbols are identified in Table 1. The dashed line represents equation (1), and  $\sigma_s$  is the thermal velocity dispersion.



**Figure 2.** The velocity dispersion  $\sigma$  plotted versus region size  $L$  for clouds containing one or more subregions in Table 1. Straight lines connect the symbols for each subregion and the larger region or cloud of which it is a part. The data shown in the left part of panel (b) are from Snell (1979), and represent velocity dispersions inferred from the linewidth only. The dashed lines represent equation (1).

case  $\sigma$  is the velocity dispersion inferred from the linewidth only, and the dots indicate subregions of different size. In nearly all clouds  $\sigma$  increases systematically with  $L$ , and the form of the  $\sigma(L)$  relation is similar to the overall  $\sigma(L)$  relation of Fig. 1. However, there appear to be some real differences between different clouds; for example, the amplitude of the  $\sigma(L)$  relation is relatively small in the Taurus complex, larger in the  $\rho$  Ophiuchus complex, and still larger in the Orion A cloud. Also, two prominent condensations closely associated with H II regions, M17SW and OMC1, stand out as exceptions to the general increase of  $\sigma$  with  $L$ ; they will be suggested in Section 4 to be regions that have undergone significant gravitational collapse.

Further evidence for a nearly universal  $\sigma(L)$  relation similar in form to equation (1) is provided by the relative magnitude of  $\sigma(V)$ , the velocity dispersion associated with variations in radial velocity  $V$  across a cloud, and  $\sigma(\Delta V)$ , the velocity dispersion inferred from the linewidth  $\Delta V$ . For a spherical cloud, it can be shown that the average distance between pairs of points randomly scattered throughout the cloud is  $54/35$  times the average separation of points confined to a single diameter or line-of-sight through the centre. If the difference in velocity between two points is correlated with their separation according to equation (1), the total velocity dispersion of the whole cloud should be  $(54/35)^{0.38} = 1.18$  times the velocity dispersion  $\sigma(\Delta V)$  along a single line-of-sight, which implies that  $\sigma(V)/\sigma(\Delta V) = (1.18^2 - 1)^{1/2} = 0.62$ . The ratio of  $\sigma(V)/\sigma(\Delta V)$  has been calculated for all regions for which sufficient data are available, and in the smaller regions with  $L < 10$  pc its geometric mean value happens to be exactly 0.62. In regions with  $L > 10$  pc the geometric mean of this ratio is about 1.7; this larger value can be understood as resulting from a filamentary or sheet-like structure of the larger clouds if their typical line-of-sight thickness is only about  $1/10$  of their total linear extent.

The fact that nearly all of the regions studied show approximately the same power-law dependence of velocity dispersion on region size suggests that the observed motions are all part of a common hierarchy of interstellar turbulent motions, and that they have no preferred length-scale, although there may be local variations in their amplitude. These

characteristics are similar to those of subsonic turbulent flows, which consist of a hierarchy of small eddies superimposed on larger ones, with a characteristic power-law dependence of eddy velocity on length scale that is the well-known Kolmogoroff law,  $\sigma \propto L^{1/3}$ . Although the motions in molecular clouds are supersonic and very little is known about supersonic turbulence, some similarities with subsonic turbulence should exist; for example, hydrodynamical instabilities may occur as in the subsonic case and generate small-scale irregularities and hence turbulence in large-scale flows (Larson 1979; Woodward 1979). There is in fact some experimental evidence that the structure of moderately supersonic turbulent shear flows is very similar to that of subsonic flows (Bradshaw 1977). The fact that the  $\sigma(L)$  relation in molecular clouds is somewhat steeper than the Kolmogoroff law seems consistent with an interpretation of the observed motions as supersonic turbulence, since in the supersonic case some of the kinetic energy of large-scale motions can be dissipated directly by shocks before being degraded into smaller-scale motions; thus there should be less energy in small-scale motions, and a steeper  $\sigma(L)$  relation than in the subsonic case.

In view of the likely importance of shock dissipation, it is perhaps remarkable that the observed relation  $\sigma \propto L^{0.38}$  is so close to the Kolmogoroff law  $\sigma \propto L^{0.33}$ . This might be explained if the observed motions in molecular clouds are actually due to subsonic or mildly supersonic turbulence in a warmer atomic medium in which the molecular gas is embedded as cool condensations. Such a situation could arise, for example, from collisions between atomic clouds, which produce thick layers of shock-heated atomic gas in which thin sheets of cold molecular gas form by thermal instabilities (Smith 1980). The molecular gas would then follow the subsonic turbulent motions that would almost certainly be present in the warmer atomic gas. A number of molecular cloud complexes are observed to be embedded in comparable amounts of atomic gas (Blitz & Shu 1980; Israel 1980; Burton, Liszt & Baker 1978), so it is plausible that the observed molecular motions could reflect motions in the atomic gas.

In addition to the processes of turbulent hydrodynamics discussed above, it is possible that some of the small-scale motions in molecular clouds are produced by stars through the effects of stellar winds, supernova explosions, or the expansion of H II regions. However, it seems unlikely that such effects could be dominant, since the resulting velocities would be largest on the smallest scales, contrary to the observed trend. Also, some of the small dark clouds included in this study contain no known young stars, and there is no evidence that they have smaller velocity dispersions than similar clouds that do contain young stars. The best evidence for a stellar energy source is provided by the broad wings of the molecular lines of the unresolved KL source in Orion, whose width of  $\sim 50 \text{ km s}^{-1}$  (e.g. Wilson, Downes & Bieging 1979) is generally attributed to mass outflow from a massive newly formed star. Most of the regions in Table 1 are not so intimately associated with massive newly formed stars, so the effects of stellar winds, etc., should be much smaller.

#### 4 Gravity in molecular clouds

As a first step in examining the possible influence of the masses of molecular clouds on their dynamics, Fig. 3 gives a plot of  $\sigma$  versus  $M$  for the same objects as shown in Fig. 1. There is a close correlation between  $\log \sigma$  and  $\log M$ , and it is well represented by the eye-fitted dashed line, whose equation is

$$\sigma (\text{km s}^{-1}) = 0.42 M(M_{\odot})^{0.20}; \quad (2)$$

the rms deviation of  $\log \sigma$  from this relation is 0.12. The scatter in Fig. 3 appears smaller than that in Fig. 1, and inspection of the plots shows that this is because some of the objects

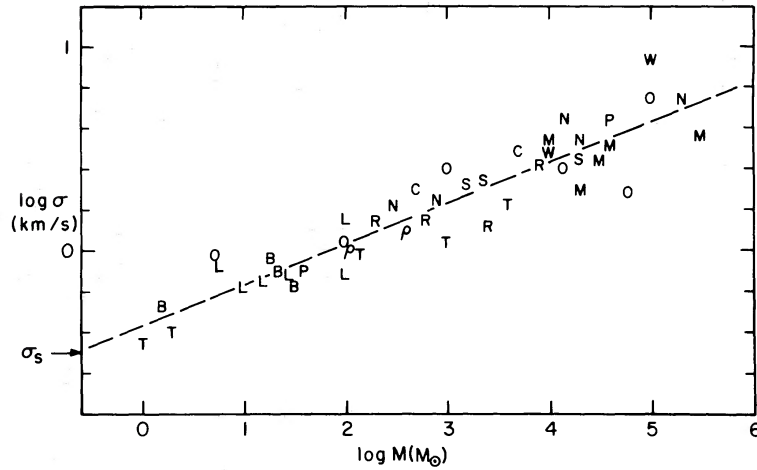


Figure 3. The velocity dispersion  $\sigma$  plotted versus total mass  $M$  for the same regions shown in Fig. 1. The dashed line represents equation (2).

that appear most discrepant in Fig. 1 lie closer to the mean relation in Fig. 3. For example, OMC1 lies 0.33 dex above the dashed line in Fig. 1 but only 0.17 dex above the line in Fig. 3; this is because it has not only a large velocity dispersion but also an unusually large mass for its size. A positive correlation between velocity dispersion and mass for a given size is just what would be expected if all of the objects studied were in approximate virial equilibrium.

For a spherical cloud of mass  $M$ , diameter  $L$  and velocity dispersion  $\sigma$ , the kinetic energy and gravitational potential energy are respectively  $\frac{1}{2}M\sigma^2$  and  $\sim -2GM^2/L$ , so that the virial theorem implies

$$\sigma^2 \sim \frac{2GM}{L} \quad (3)$$

This equation would be exact for a polytrope of index  $n = 2$ , and should be valid within a factor of 2 for most clouds of different shapes and degrees of central concentration. The ratio  $2GM/\sigma^2L$  has been calculated for all of the objects in Figs 1 and 3, and is given in Table 1 and plotted logarithmically versus  $L$  in Fig. 4. The dashed line in this figure is not fitted to the points, but represents the relation

$$\frac{2GM}{\sigma^2L} = 0.92L \text{ (pc)}^{0.14} \quad (4)$$

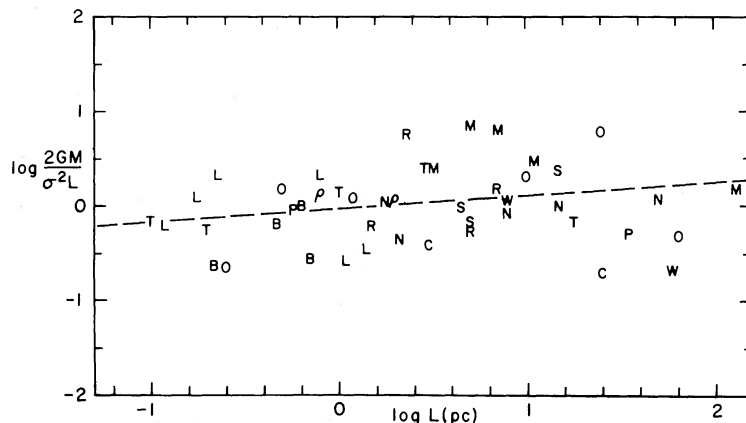


Figure 4. The virial ratio  $2GM/\sigma^2L$  plotted versus region size  $L$  for the same regions shown in Figs 1 and 3. The dashed line represents equation (4), and is derived from equations (1) and (2).

derived from equations (1) and (2). The plotted values of  $\log(2GM/\sigma^2L)$  show no significant correlation with  $L$ , and their mean value is  $-0.02$ , showing that on the average equation (3) is closely satisfied. The standard deviation of  $\log(2GM/\sigma^2L)$  is  $0.39$ , which seems consistent with the estimated errors in  $M$ ,  $L$  and  $\sigma$ , especially the error in  $M$  which is probably typically a factor of 2. We can therefore conclude that most of the regions studied are gravitationally bound and at least approximately in virial equilibrium. Previous authors have noted that the virial theorem is roughly satisfied in some individual objects; for example, Elmegreen, Lada & Dickinson (1979) have noted that it is approximately valid for the various subregions of the M17 complex.

It is plausible that approximate virial balance should exist, or should soon be attained, in molecular clouds if they consist of many independently moving clumps or subregions; the observed internal velocities would then be sufficient to support most clouds against overall collapse. However, it cannot be ruled out that some clouds are actually collapsing, since even in the extreme case of free-fall collapse the velocities generated would not differ from equilibrium velocities by more than about a factor of  $\sqrt{2}$ . The turbulent nature of the observed motions implies that gravitational collapse cannot occur as a simple radial free fall, but must be strongly modified and perhaps retarded by the turbulent motions; the virial theorem might then remain closely satisfied. In any case, Fig. 4 shows that objects of a wide range of sizes, including the subcondensations in larger clouds, are similarly close to a state of virial balance, as judged by the near constancy of the ratio  $2GM/\sigma^2L$ .

If dissipation of turbulent motions occurs and causes a cloud to contract while still remaining nearly in virial equilibrium, this will reduce the size of the cloud and increase its internal velocity dispersion. Gravitational contraction could therefore account for some of the scatter in the  $\sigma(L)$  relation in Figs 1 and 2. For example, OMC1 and M17SW have unusually high velocity dispersions falling at the upper edge of the scatter in Fig. 1, and it is plausible that they have undergone significant gravitational contraction because they are the densest parts of larger clouds and are the sites of formation of massive stars. The largest deviation from the average  $\sigma(L)$  relation occurs for the extremely compact and dense KL core region of OMC1 (see Fig. 2a), where the effects of collapse and star formation are most evident. However, most regions deviate much less from the average  $\sigma(L)$  relation, and this suggests that they have not undergone significant free gravitational collapse; if the scatter in Fig. 1 is interpreted as having been produced by varying amounts of gravitational contraction, the required maximum shrinkage in overall size is less than a factor of 2.

If most of the regions studied have not undergone significant gravitational collapse, the observed clumpy structure of molecular clouds must have been produced by other processes. The existence of a nearly universal  $\sigma(L)$  relation, and the generally irregular and filamentary appearance of molecular clouds and their substructures, suggest that processes of turbulent hydrodynamics have played an important role in their formation. Since the turbulent motions in molecular clouds are generally supersonic, shock compression and associated hydrodynamical instabilities (e.g. Woodward 1979) are likely to occur and produce condensed structures such as sheets, filaments or clumps within the clouds. Most of these structures will probably be quite transient, but some may be massive and dense enough to be gravitationally bound, in which case their self-gravity will help to maintain their existence. A hierarchy of bound condensations of different sizes might then result if hydrodynamical processes generate compressed regions with a wide range of sizes and densities, and gravity selects and preserves those that happen to be gravitationally bound.

In reality, there may not be such a clear division between the roles of hydrodynamics and gravity, and they may work together to produce the observed structures. For example, gravity may help to drive the supersonic motions that compress the gas, while the motions

on different length-scales remain coupled by processes of turbulent hydrodynamics. Eventually, some regions may become so condensed that they no longer interact much with their surroundings, and they collapse independently with increasing internal velocity dispersions, as suggested above for regions like M17SW and OMC1.

## 5 Density structure of molecular clouds

If molecular clouds have velocity dispersions that depend on size according to equation (1), the smaller clouds must have higher densities to be gravitationally bound. To demonstrate directly the correlation between density and size, average densities have been calculated for all of the regions whose masses are known, and they are listed in Table 1 and plotted versus region size in Fig. 5. The average density is defined as that of a sphere of mass  $M$  and diameter  $L$ , and is expressed in terms of  $n(\text{H}_2)$ , the number of  $\text{H}_2$  molecules per  $\text{cm}^3$ . The dashed line in Fig. 5 is not fitted to the points but represents the relation

$$\langle n(\text{H}_2) \rangle (\text{cm}^{-3}) = 3400 L (\text{pc})^{-1.10} \quad (5)$$

derived by eliminating  $\sigma$  from equations (1) and (2). Equation (5) represents well the general trend of the data, except for some of the largest cloud complexes which have lower mean densities. Most of these regions also have lower than average values of  $2GM/\sigma^2 L$  in Fig. 4, and a plausible explanation is that many large molecular complexes contain comparable amounts of atomic gas whose mass is not included in the values listed in Table 1 (Blitz & Shu 1980).

The average densities plotted in Fig. 5 vary from  $\sim 10 \text{ cm}^{-3}$  for the largest complexes to  $\sim 10^5 \text{ cm}^{-3}$  for the smallest clumps, spanning the entire range from the densities of 'standard HI clouds' to the densities expected for protostars. The correlation  $\langle n(\text{H}_2) \rangle \propto L^{-1.1}$  may have implications for the origin of the observed structures, since it implies that the column density  $\langle n(\text{H}_2) \rangle L$  varies only as  $L^{-0.1}$  and therefore is nearly independent of size; this near constancy of  $nL$  could result, for example, from one-dimensional shock-compression processes which preserve the column density of the regions so compressed. Another possibility might be that optical depth plays an important role in the formation and survival of molecular clouds, and that this results in a favoured range of optical depths; the visual extinction implied by equation (5) varies only from about 7 mag for  $L = 100 \text{ pc}$  to 13 mag

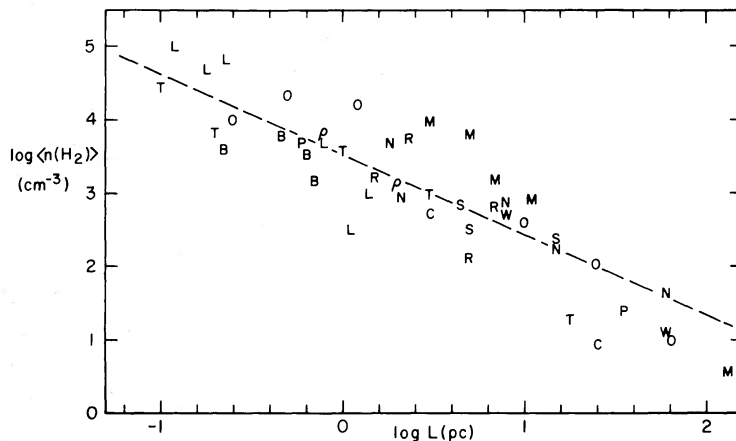


**Figure 5.** The average density, defined as the density of a sphere of mass  $M$  and diameter  $L$ , of all the regions shown in Figs 1 and 3 plotted versus region size  $L$ . The dashed line represents equation (5), and is derived from equations (1) and (2).

for  $L = 0.1$  pc. Finally, the correlation in Fig. 5 could also be produced partly by observational selection effects if only a limited range of column densities can be detected by the available techniques. If the processes that form molecular clouds do tend to generate structures with  $nL \sim \text{constant}$ , and if the virial theorem also holds, this would imply  $\sigma \propto L^{1/2}$ , not greatly different from the observed relation. Again it may not be possible to completely disentangle such effects from the processes of turbulence discussed above, but the fact that the  $\sigma(L)$  relation in Fig. 1 seems better defined than the  $n(L)$  relation in Fig. 5 suggests that turbulent processes may be more fundamental than the above effects.

## 6 Possible implications for star formation

### 6.1 THE ORIGIN OF PROTOSTARS

Since the observed condensations in molecular clouds are gravitationally bound, they may play a role in, or represent a stage in, star formation. Many of the smaller condensations have masses in the stellar mass range, so they may actually be protostars. In support of this possibility, the smallest object in Figs 1 and 3, TMC2 (Myers, Ho & Benson 1979), has properties remarkably similar to those of a 'theorist's protostar': its mass is  $\sim 1 M_{\odot}$  and its diameter is  $\sim 0.1$  pc, nearly identical to that of the  $1 M_{\odot}$  protostar model of Larson (1969). Protostars may thus be part of the hierarchy of bound structures in molecular clouds, and may be formed by the processes of turbulent hydrodynamics discussed in Sections 3 and 4.

TMC1 and TMC2 are the only objects listed in Table 1 whose internal motions are subsonic, so that the dominant contribution to  $\sigma$  comes from thermal motions. If smaller-scale structure is produced by supersonic internal motions, as suggested in Section 4, then objects like TMC1 and TMC2 may not possess or develop much internal substructure; moreover, since they nearly satisfy the Jeans criterion, they should not undergo much fragmentation if they collapse gravitationally (Larson 1972, 1978; Tohline 1980; Bodenheimer, Tohline & Black 1980). These objects may therefore be almost the smallest bound structures that can be formed, either by hydrodynamical processes or by gravitational collapse.

If the hierarchy of subcondensations in molecular clouds terminates with objects so small that their internal motions are no longer supersonic, we can estimate the minimum clump size by putting  $\sigma = \sigma_s = 0.32 \text{ km s}^{-1}$  (for  $T = 10 \text{ K}$ ) in equations (1) and (2). This predicts as typical minimum values  $L = 0.04$  pc and  $M = 0.25 M_{\odot}$ , slightly smaller than the size and mass of the smallest objects yet directly resolved by molecular line observations. Taking into account the rms scatter in the  $\sigma(L)$  and  $\sigma(M)$  relations, a one-standard-deviation range of values for the minimum clump size and mass is predicted to be  $0.015 \lesssim L \lesssim 0.1$  pc and  $0.05 \lesssim M \lesssim 1.0 M_{\odot}$ . TMC2 falls at the upper end of this range, which is consistent with the fact that the velocity dispersions in the Taurus clouds are about one standard deviation below the mean  $\sigma(L)$  and  $\sigma(M)$  relations. If clumps of the predicted minimum size collapse without fragmentation and with high efficiency to form single stars, a lower stellar mass limit in the range  $0.05 \lesssim M \lesssim 1.0 M_{\odot}$  is predicted; if some fragmentation occurs, for example into binary or multiple systems, somewhat smaller masses would result. A reasonable expectation might be that the stellar mass spectrum should begin to turn downward for masses less than  $0.1 M_{\odot}$ ; this expectation is consistent with the available data for the local stellar mass spectrum (Miller & Scalo 1979). Fragmentation theories, by contrast, provide no natural reason why fragmentation should stop with masses in the observed stellar mass range and not continue down to masses of  $\sim 10^{-2} M_{\odot}$ , the limit set by opacity (Low & Lynden-Bell 1976).

The formation of massive stars, on the other hand, must be a more complicated process than in the existing protostellar collapse models, since the data in Table 1 and Fig. 3 show

that all regions with masses  $\geq 10 M_{\odot}$  have supersonic internal motions with  $\sigma > 2\sigma_s$ . These supersonic motions can be expected to generate smaller-scale internal structure; moreover, since the number of Jeans masses present is at least  $(\sigma/\sigma_s)^3$  or  $2.3 (M/M_{\odot})^{0.60}$  from equation (2), fragmentation into at least this number of smaller clumps would be expected to occur even in the absence of initially supersonic motions (Larson 1978). Interactions and accumulation processes, including coalescence of clumps and accretion of diffuse gas by them, will probably play an important role in the formation of massive stars in such regions (Silk 1978; Larson 1978). Since many stars are almost certainly formed, massive stars should generally occur only as members of clusters or associations, in agreement with what is actually observed. Thus, for massive stars, the concept of an isolated protostar of well-defined mass that collapses to form a single star is probably not realistic.

The important role of supersonic turbulence and accumulation processes for star formation was first recognized by McCrea (1960, 1978), who suggested that stars form by the accumulation of many small 'floccules'. The present picture for massive stars is similar in some respects to McCrea's floccule theory, although the 'floccules' considered here are much larger than those postulated by McCrea, and are gravitationally bound objects.

## 6.2 THE STELLAR MASS SPECTRUM

If most stars form by accretional build-up processes in clouds containing many pre-stellar condensation nuclei, the final stellar mass spectrum may be determined by the outcome of competition between different condensations to accrete the remaining matter in the cloud. This will produce a large spread in the final masses, since the condensations that happen to start out largest will accrete fastest and undergo a runaway growth in mass relative to the smaller ones; some of the smaller objects may even be accreted by larger ones. Such processes tend to create a hierarchy of a few large objects and many small ones, with a mass spectrum that is asymptotically of power-law form, since there is no preferred mass. For example, the coagulation models studied by Silk & Takahashi (1979) predict mass spectra that are asymptotically of the form

$$\frac{dN}{d \log M} \propto M^{-x} \quad (6)$$

where  $0 \leq x \leq 1$ . A numerical simulation of protostellar coalescence by Arny & Weissman (1973) yielded an approximate power-law mass spectrum with  $x \sim 0.7$ , in rough agreement with the predicted value  $x = 0.5$  for their adopted assumptions. The accretion of diffuse gas by objects of different mass also leads to a power-law mass spectrum, with  $x = 1$  (Zinnecker 1980). Both types of accretion processes occur in the simulations by Larson (1978) of collapse and fragmentation, in which the final masses of the objects formed are established largely by accretional build-up; in this case the spatial distribution of the objects formed suggests a tendency toward a self-similar satellite or binary hierarchy, which again predicts a power-law mass spectrum with  $x \leq 1$ .

Theories that predict power-law spectra with  $x \sim 1$  can claim reasonable agreement with observations (Tinsley 1978), although the solar-neighbourhood IMF is not exactly a power law but has a slope that increases with mass as  $x = 1 + \log M$ , according to Miller & Scalo (1979). The implied turnover in the IMF at masses  $< 0.1 M_{\odot}$  is consistent with the minimum protostellar mass predicted in Section 6.1, and the increasingly steep decline at high masses is plausibly attributable to the difficulty in forming very massive stars by accretion (Larson & Starrfield 1971; Kahn 1974; Yorke & Krügel 1977). Thus, although a quantitative prediction of the IMF cannot yet be made, it may at least be possible to identify some of the important physical processes that determine it.

If small stars form directly in small molecular clumps while massive stars form only by accretional build-up in much more massive clouds, small stars should form widely throughout molecular clouds of all sizes, while massive stars should form only in the densest parts of the most massive clouds. This expectation is consistent with observations: in Taurus, low-mass young stars are scattered widely throughout filamentary clouds containing many small clumps, while in Orion massive newly formed stars are also present and are associated with the densest parts of the Orion clouds, which are much more massive than the Taurus clouds. Thus the IMF for massive stars appears to depend on cloud properties in that it extends to higher masses in the more massive and condensed clouds. A possible implication of this might be that the formation of massive stars is more localized in spiral arms than the formation of lower-mass stars (Larson 1977b).

The argument of Section 6.1 predicts that the low-mass part of the IMF also depends on cloud properties, in this case on the temperature and on the magnitude of turbulent velocities. If the strength of turbulence can be characterized by a parameter  $\sigma_0$  such that  $\sigma = \sigma_0 M^{0.20}$ , as in equation (2), then the minimum protostellar mass obtained by setting  $\sigma = \sigma_s$  is  $M_{\min} = 0.25 (\sigma_0/0.42)^{-5} (T/10)^{2.5} M_\odot$ . The parameter  $\sigma_0$  appears to be significantly different in different clouds (Figs 1–3), and there is some suggestion from the data that it may be larger in the more massive clouds, resulting in smaller values of  $M_{\min}$ . On the other hand, the temperature  $T$  also tends to be higher in the more massive clouds, and this has the effect of increasing  $M_{\min}$ . A prediction of the behaviour of the lower IMF therefore awaits a more complete study of the properties of molecular clouds, including their temperatures. Meanwhile we note that it may be possible to apply these considerations to globular clusters, all of which have comparable masses and velocity dispersions, so that  $\sigma_0$  may not have been very different in different proto-globular clusters. The important parameter is then the gas temperature, which increases with decreasing abundance of the heavy elements; consequently, the turnover mass should increase and the IMF should be progressively more depleted in low-mass stars in clusters of decreasing heavy-element content. This expectation is consistent with the available data on the IMF in globular clusters (Freeman 1977; Da Costa 1980).

## 7 Possible implications for the origin and evolution of molecular clouds

Associated with the observed internal motions there is a time-scale  $\tau \sim L/\sigma$  for large changes in the structure of a molecular cloud;  $\tau$  is about twice the free-fall time. During this time appreciable dissipation of turbulent motions will occur, and gravitational collapse and star formation will probably also occur in at least some parts of the cloud, resulting in partial or complete dispersal or restructuring of the cloud by the effects of stellar winds, H II regions, etc. The time-scale  $\tau$  estimated from equation (1) is  $\tau(\text{yr}) \sim 10^6 L(\text{pc})^{0.62}$ , and varies from about  $2 \times 10^5$  yr for  $L = 0.1$  pc to  $1.5 \times 10^7$  yr for  $L = 100$  pc. Thus even the largest molecular cloud complexes must be rather transient and will be completely restructured, if not completely dispersed, after only a few times  $10^7$  yr. Evidence that molecular clouds have life-times of this order is provided by the fact that molecular gas is seldom seen in the close vicinity of star clusters whose ages are greater than about  $10^7$  yr (Bash, Green & Peters 1977), and the fact that the largest spread in stellar ages observed in associations of young stars is about  $10^7$  yr (Blaauw 1964; Cohen & Kuhl 1979).

The existence of such a short cloud lifetime (see also Elmegreen 1979; Blitz & Shu 1980; Cohen *et al.* 1980) implies that molecular clouds are continually being formed or reassembled out of atomic or molecular gas by processes whose time-scale does not exceed a few times  $10^7$  yr. Thus, for example, the models proposed by Kwan (1979) and Scoville &

Hersh (1979), in which molecular clouds are built up by random collisions and coalescence of smaller clouds, are not quantitatively adequate because they predict growth times of  $\geq 2 \times 10^8$  yr. This does not necessarily mean that the idea of collisional cloud growth is incorrect, but it does mean that *random* cloud collisions are not adequate and that more systematic motions are required. Such systematic motions would be expected in a turbulent picture of the interstellar medium, since turbulent motions are not random but consist of small-scale irregularities superimposed on larger-scale, more systematic flows with larger velocities. The formation of molecular clouds probably requires motions with length scales of a few hundred parsecs, velocities of  $\sim 10 \text{ km s}^{-1}$ , and time-scales of a few times  $10^7$  yr, and an important problem for further research will be to understand better the nature and origin of these motions.

## 8 Conclusions

The internal velocity dispersions of molecular clouds are well correlated with their sizes and masses, and similar correlations hold even for the different subregions of an individual cloud or complex. The  $\sigma(L)$  relation thus found is essentially the same as that for interstellar motions on larger scales, and is not greatly different from the Kolmogoroff law  $\sigma \propto L^{1/3}$  for subsonic turbulence. This suggests that the internal motions in molecular clouds are part of a general hierarchy of interstellar turbulent motions. The apparent similarity between these motions and subsonic turbulence may result if molecular clouds form as cold condensations in warmer atomic gas, and if their motions arise from subsonic or mildly supersonic turbulence in the warmer gas.

Essentially all of the molecular condensations studied are gravitationally bound, and they approximately satisfy the virial theorem. Some of the densest parts of larger clouds, such as OMC1, may have undergone significant gravitational contraction, but the moderate scatter in the  $\sigma(L)$  relation implies that most regions have not collapsed very much since they were formed. This argues against the simplest picture of gravitational collapse and fragmentation, and suggests that processes of turbulent hydrodynamics have played an important role, along with gravity, in producing the observed substructures in molecular clouds.

The smallest clumps in molecular clouds have properties very similar to those expected for low-mass protostars. If the subcondensations in molecular clouds are produced by supersonic hydrodynamics, the hierarchy of clumps of various sizes may terminate with objects so small that their internal velocities are no longer supersonic; this is predicted to occur for masses that are typically a few tenths of a solar mass. If these minimum-size clumps collapse and form stars of comparable mass, this would account for the apparent turnover of the stellar mass function at low masses.

Clumps large enough to form massive stars must evolve in a more complex fashion, since they always have supersonic internal motions and often show a complex internal structure. These massive clumps probably form groups or clusters of stars, and the most massive stars are probably built up by accretion from smaller pre-stellar condensations. The fact that the most massive stars appear to form only in the densest parts of the most massive clouds also suggests that accumulation processes are involved. Theories and numerical simulations in which stars are formed by accretion processes can predict roughly the correct form for the stellar mass function, although a detailed prediction will eventually have to consider the dependence of the IMF on cloud properties such as mass, strength of turbulence and temperature.

The magnitude of the observed internal motions implies that the structure of molecular clouds must be quite transient, changing completely after  $\sim 10^7$  yr; empirical evidence suggests that clouds are dispersed after this time. Random collisions of smaller clouds cannot

build up molecular clouds in such a short time, and more systematic motions on a scale of at least a few hundred parsecs are required; presumably these motions are closely related to those that produce spiral structure in galaxies. A better knowledge of the dynamical processes responsible for the formation of molecular clouds will be essential for any improved understanding of star formation.

### Acknowledgments

Informative discussions with L. Blitz, P. T. P. Ho, P. C. Myers, A. A. Penzias, J. A. Smith, J. E. Smith, J. E. Tohline, P. R. Woodward and H. Zinnecker have provided valuable guidance for the work reported here. Helpful comments by B. M. Tinsely led to improvements in the manuscript.

### References

- Army, T. & Weissman, P., 1973. *Astr. J.*, **78**, 309.
- Bash, F. N., Green, E. & Peters, W. L., 1977. *Astrophys. J.* **217**, 464.
- Bechis, K. P., Harvey, P. M., Campbell, M. F. & Hoffman, W. F., 1978. *Astrophys. J.*, **226**, 439.
- Blaauw, A., 1964. *A. Rev. Astr. Astrophys.*, **2**, 213.
- Blair, G. N., Evans, N. J., Vanden Bout, P. A. & Peters, W. L., 1978. *Astrophys. J.*, **219**, 896.
- Blitz, L., 1980. In preparation.
- Blitz, L. & Shu, F. H., 1980. *Astrophys. J.*, **238**, 148.
- Bodenheimer, P. & Black, D. C. 1978. In *Protostars and Planets, IAU Colloquium No. 52*, p. 288, ed. Gehrels, T., University of Arizona Press, Tucson.
- Bodenheimer, P., Tohline, J. E. & Black, D. C. 1980. Preprint.
- Bradshaw, P., 1977. *A. Rev. Fluid Mech.*, **9**, 33.
- Burton, W. B., Liszt, H. S. & Baker, P. L., 1978. *Astrophys. J.*, **219**, L67.
- Caldwell, J. A. R., 1979. *Astr. Astrophys.*, **71**, 255.
- Churchwell, E., Winnewisser, G. & Walmsley, C. M., 1978. *Astr. Astrophys.*, **67**, 139.
- Cohen, M. & Kuhl, L. V., 1979. *Astrophys. J. Suppl.*, **41**, 743.
- Cohen, R. S., Cong, H., Dame, T. M. & Thaddeus, P., 1980. *Astrophys. J.*, **239**, L53.
- Crutcher, R. M., Hartkopf, W. I. & Giguere, P. T., 1978. *Astrophys. J.*, **226**, 839.
- Da Costa, G., 1980. In preparation.
- Dickel, H. R., Dickel, J. R. & Wilson, W. J., 1977. *Astrophys. J.*, **217**, 56.
- Dickman, R. L., 1978. *Astrophys. J. Suppl.*, **37**, 407.
- Elmegreen, B. G., 1979. *Astrophys. J.*, **231**, 372.
- Elmegreen, D. M. & Elmegreen, B. G., 1978. *Astrophys. J.*, **220**, 510.
- Elmegreen, D. M. & Elmegreen, B. G., 1979. *Astr. J.*, **84**, 615.
- Elmegreen, B. G., Lada, C. J. & Dickinson, D. F., 1979. *Astrophys. J.*, **230**, 415.
- Evans, N. J., 1980. In *Interstellar Molecules, IAU Symposium No. 87*, ed. Andrew, B. H., D. Reidel, Dordrecht, in press.
- Evans, N. J., Blair, G. N. & Beckwith, S., 1977. *Astrophys. J.*, **217**, 448.
- Few, R. W. & Booth, R. S., 1979. *Mon. Not. R. astr. Soc.*, **188**, 181.
- Field, G. B., 1978. In *Protostars and Planets, IAU Colloquium No. 52*, p. 243, ed. Gehrels, T., University of Arizona Press, Tucson.
- Freeman, K. C., 1977. In *The Evolution of Galaxies and Stellar Populations*, p. 133, eds Tinsley, B. M. & Larson, R. B., Yale University Observatory, New Haven.
- Heiles, C. & Gordon, M. A., 1975. *Astrophys. J.*, **199**, 361.
- Heiles, C. & Katz, G., 1976. *Astr. J.*, **81**, 37.
- Ho, P. T. P., Barrett, A. H., Myers, P. C., Matsakis, D. N., Cheung, A. C., Chui, M. F., Townes, C. H. & Yngvesson, K. S., 1979. *Astrophys. J.*, **234**, 912.
- Hoyle, F., 1953. *Astrophys. J.*, **118**, 513.
- Hunter, C., 1967. In *Relativity Theory and Astrophysics, Vol. 2, Galactic Structure*, p. 169, ed. Ehlers, J., American Mathematical Society, Providence.
- Israel, F. P., 1980. Preprint.
- Jeans, J. H., 1929. *Astronomy and Cosmogony*, Cambridge University Press (reprinted by Dover, New York, 1961).

- Jones, B. F. & Herbig, G. H., 1979. *Astr. J.*, **84**, 1872.
- Kahn, F. D., 1974. *Astr. Astrophys.*, **37**, 149.
- Kutner, M. L., Tucker, K. D., Chin, G. & Thaddeus, P., 1977. *Astrophys. J.*, **215**, 521.
- Kwan, J., 1979. *Astrophys. J.*, **229**, 567.
- Lada, C. J., 1976. *Astrophys. J. Suppl.*, **32**, 603.
- Lada, C. J., Elmegreen, B. G., Cong, H.-I. & Thaddeus, P., 1978. *Astrophys. J.*, **226**, L39.
- Lang, K. R. & Willson, R. F., 1979. *Astrophys. J.*, **227**, 163.
- Larson, R. B., 1969. *Mon. Not. R. astr. Soc.*, **145**, 271.
- Larson, R. B., 1972. *Mon. Not. R. astr. Soc.*, **156**, 437.
- Larson, R. B., 1977a. In *Star Formation, IAU Symposium No 75*, p. 249, eds de Jong, T. & Maeder, A., D. Reidel, Dordrecht.
- Larson, R. B., 1977b. In *The Evolution of Galaxies and Stellar Populations*, p. 97, eds Tinsley, B. M. & Larson, R. B., Yale University Observatory, New Haven.
- Larson, R. B., 1978. *Mon. Not. R. astr. Soc.*, **184**, 69.
- Larson, R. B., 1979. *Mon. Not. R. astr. Soc.*, **186**, 479.
- Larson, R. B. & Starrfield, S., 1971. *Astr. Astrophys.*, **13**, 190.
- Liszt, H. S., Wilson, R. W., Penzias, A. A., Jefferts, K. B., Wannier, P. G. & Solomon, P. M., 1974. *Astrophys. J.*, **190**, 557.
- Little, L. T., Macdonald, G. H., Riley, P. W. & Matheson, D. N., 1979. *Mon. Not. R. astr. Soc.*, **188**, 429.
- Loren, R. B., 1976. *Astrophys. J.*, **209**, 466.
- Loren, R. B., 1977. *Astrophys. J.*, **215**, 129.
- Loren, R. B., 1979. *Astrophys. J.*, **227**, 832.
- Low, C. & Lynden-Bell, D., 1976. *Mon. Not. R. astr. Soc.*, **176**, 367.
- Lucas, R., Le Squéren, A. M., Kazès, I. & Encrenaz, P. J., 1978. *Astr. Astrophys.*, **66**, 155.
- Martin, R. N. & Barrett, A. H., 1978. *Astrophys. J. Suppl.*, **36**, 1.
- Mattila, K., Winnberg, A. & Grasshoff, M., 1979. *Astr. Astrophys.*, **78**, 275.
- McCrea, W. H., 1960. *Proc. R. Soc. Lond. A*, **256**, 245.
- McCrea, W. H., 1978. In *The Origin of the Solar System*, p. 75, ed. Dermott, S. F., Wiley, New York.
- Miller, G. E. & Scalo, J. M., 1979. *Astrophys. J. Suppl.*, **41**, 513.
- Milman, A. S., 1975. *Astrophys. J.*, **202**, 673.
- Minn, Y. K. & Greenberg, J. M., 1975. *Astrophys. J.*, **196**, 161.
- Minn, Y. K. & Greenberg, J. M., 1979. *Astr. Astrophys.*, **77**, 37.
- Myers, P. C., Ho, P. T. P., Schneps, M. H., Chin, G., Pankonin, V. & Winnberg, A., 1978. *Astrophys. J.*, **220**, 864.
- Myers, P. C., Ho, P. T. P. & Benson, P. J., 1979. *Astrophys. J.*, **233**, L141.
- Penzias, A. A., 1975. In *Atomic and Molecular Physics and the Interstellar Matter*, p. 373, ed. Balian, R., Encrenaz, P. & Lequeux, J., North Holland, Amsterdam.
- Phillips, T. G., Huggins, P. J., Wannier, P. G. & Scoville, N. Z., 1979. *Astrophys. J.*, **231**, 720.
- Sargent, A. I., 1977. *Astrophys. J.*, **218**, 736.
- Sargent, A. I., 1979. *Astrophys. J.*, **233**, 163.
- Scoville, N. Z. & Hersh, K., 1979. *Astrophys. J.*, **229**, 578.
- Silk, J., 1978. In *Protostars and Planets, IAU Colloquium No. 52*, p. 172, ed. Gehrels, T., University of Arizona Press, Tucson.
- Silk, J. & Takahashi, T., 1979. *Astrophys. J.*, **229**, 242.
- Smith, J. A., 1980. *Astrophys. J.*, **238**, 842.
- Snell, R. L., 1979. *PhD thesis*, University of Texas.
- Stark, A. A. & Blitz, L., 1978. *Astrophys. J.*, **225**, L15.
- Tinsley, B. M., 1978. In *Structure and Properties of Nearby Galaxies, IAU Symposium No. 77*, p. 15, eds Berkhuijsen, E. M. & Wielebinski, R., D. Reidel, Dordrecht.
- Tohline, J. E., 1980. *Astrophys. J.*, **235**, 866.
- Wilson, T. L., Downes, D. & Bieging, J., 1979. *Astr. Astrophys.* **71**, 275.
- Wilson, T. L. & Minn, Y. K., 1977. *Astr. Astrophys.*, **54**, 933.
- Woodward, P. R., 1978. *A. Rev. Astr. Astrophys.*, **16**, 555.
- Woodward, P. R., 1979. In *The Large-Scale Characteristics of the Galaxy, IAU Symposium No. 84*, p. 159, ed. Burton, W. B., D. Reidel, Dordrecht.
- Yorke, H. W. & Krügel, E., 1977. *Astr. Astrophys.* **54**, 183.
- Zinnecker, H., 1980. In preparation.
- Zuckerman, B. & Palmer, P., 1974. *A. Rev. Astr. Astrophys.*, **12**, 279.

**Note added in proof**

A recent numerical simulation of the Kelvin–Helmholtz instability in a supersonic shear flow by T. Tajima and J. N. Leboeuf (1980, *Phys. Fluids*, **23**, 884) shows the development of turbulence characterized by wavy filaments or streamers closely resembling the structures often seen in molecular clouds; this result supports the interpretation of the observed structures and motions in terms of hydrodynamical instabilities and turbulence.